

Size effect in splitting tests on plain and steel fiber-reinforced concrete: A non-local damage analysis

Liberato Ferrara

Department of Structural Engineering, Politecnico di Milano, Italy

Ravindra Gettu

Department of Construction Engineering, Universitat Politècnica de Catalunya, Spain

ABSTRACT: Recent splitting-tension tests on plain and steel fiber reinforced concrete have shown that, besides the existence of a size effect that depends on the relative width of the loading area, the deformations due to the splitting and compression (including the consequent wedge development) can be uncoupled through tests of whole and previously-halved discs. In order to have a better insight into the problem, experiments have been analysed through a non-local damage model. The material properties were first identified using three-point bending test data from geometrically-similar notched beams. Numerical analyses of the splitting tests, both in the traditional and modified test configurations, were then performed with a two-fold purpose. On one hand, it aims at a better understanding of the splitting test, as well as the reliability of jointly using the two types of tests for obtaining the fracture parameters for both plain and fiber concretes. On the other hand, the applicability of the proposed modeling tool is thoroughly checked.

1 INTRODUCTION

The splitting tensile test, conceived independently by Akazawa, in Japan (see RILEM, 1953) and by Carneiro and Barcellos in Brazil (1953) has been accepted by several standards as a test for measuring the tensile strength of concrete. The reason for such universal acceptance is due to its simplicity, as well as the possibility of using the same cylinder specimens as those used for the measurement of the compressive strength. From the beginning, researchers have been interested in the analysis of the test. In an early study by Wright (1955), for example, the correlation between the results from such a test and other direct or indirect tensile test methods was looked into. Furthermore the influence of boundary conditions (i.e., size and stiffness of the loading strips), on the tests results, as well as the specimen size was also investigated. Later studies (Nilsson, 1961; Ramakrishnan et al., 1967; Davies and Bose, 1968) investigated, through tests and finite element linear elastic analyses, the different geometries of splitting tests: discs, cubes, prisms and diagonally-compressed cubes. Later, Chen and Chen (1976), and Chen and Yuan (1978), by means of different approaches based on the plasticity field theory, showed that the "plastic" stress distribution differs from the elastic one by no more than 14% and that the elastic solution lies between the upper and lower bound plastic solutions. Such a result, which is not common to all test geometries, confirmed the reliability of the elastic formula $\sigma = 2P/\pi bd$, employed

to compute the equivalent tensile strength of concrete from the maximum load in the splitting test. Ojdrovic and Petroski (1987) were the first to study the behaviour of the split-cylinder test from the point of view of fracture mechanics. They employed both conventional specimens and specimens with precast diametral notches of various sizes, arguing that the behaviour of such a specimen – where the stress concentration ahead of the notch tip is superimposed on the nearly uniform tensile stress field along the diameter – is similar to that of the conventional specimen after the crack has formed and is propagating. They clearly identified the "correct" sequence of failure mechanisms in the specimen: a crack first starts to develop somewhere in the uniform tensile zone and then propagates toward the loading points. Only after the central crack is completely formed (i.e., the cylinder is split into two halves), the secondary cracking occurs at the loading strips, leading to the separation of the two halves. Three main stages can, therefore, be identified in the load-CMOD curves: an initial linear elastic part followed by a nonlinear one, which is representative of the micro- and macrocrack propagation up to the splitting of the cylinder into two halves, and, finally, an almost-flat plateau, which can be regarded as a characteristic of the structural system represented by the two "column-like" halves. For unnotched specimens the linear part extends almost up to the peak, with brittle failure. Similar failure occurs for small relative notch lengths (0.1-0.2), where the final load, i.e., the load sustained by the two specimen halves,

appears to be lower or almost equal to that at the onset of the nonlinear stage, as well as the maximum load. For longer notches the deviation from linearity occurs earlier, the stress concentration ahead of the notch tip is higher and a progressively lower load is required to initiate microcrack formation. However, the stored energy is not sufficient to cause specimen separation or to reach the load-bearing capacity. This results in a maximum load that is almost independent of the notch size. Such an existence of a "primary peak load", due to the diametral tensile strength, and of a secondary peak load, related to the load bearing capacity of the two half-disks, were also used by Bazant et al. (1991) to explain the size-dependence in their results, as well as those of Haze-gawa et al. (1985). If the first value is larger than the second, the specimen undergoes brittle failure, which is likely to exhibit size effect; otherwise plastic or ductile failure occurs, which results in size independent behavior and the corresponding bearing capacity is a lower limit of the nominal stress at failure of the split disk. Such results led to the modification of Bazant's size effect law with an additional term for taking the secondary load bearing mechanism into account.

Rocco et al. (1999, a-c) recently provided an extensive report of both analytical and experimental work done on this subject. Following the entire crack propagation with a video camera, they confirmed that cracking starts at the middle of the specimen and then propagates to the loading strips. Once the central crack has extended all along the symmetry plane, secondary cracking starts and propagates symmetrically up to failure, which occurs when one among the four secondary cracks reaches the diametral one. The effect of the width of the loading strips was also considered, whose increase is likely to raise the measured tensile strength and also the ratio between the secondary load-bearing capacity and the maximum load. As far as the effect of size effect is considered, results by Rocco et al. (1999b) are likely to confirm the modified Bazant's law; also the ratio between the secondary peak and the maximum load was found to decrease with the specimen diameter.

The problem was also recently reconsidered by Carmona (1997; also Carmona et al., 1998), where entire and previously halved circular specimens of different sizes (see also Hannant et al. 1973) were tested in order to uncouple the two different bearing mechanisms. The sequence of the primary and secondary rupture mechanisms was similar to that mentioned above. They also observed the slight decrease in secondary peak/maximum load ratio with the size of the disk. Their results have been analyzed in this paper, in order to get a better insight into the problem, by means of a non-local damage model.

2 MATERIAL MODELLING HYPOTHESES AND PARAMETER CALIBRATION USING THREE POINT BENDING TESTS

The "Crush-Crack" non-local damage model (di Prisco and Mazars, 1996) actually couples elastic stiffness degradation – as in the classical framework of Continuum Damage Mechanics – with the accumulation of both irreversible tensile and compressive strains. The evolution of the latter is regarded as completely uncoupled with respect to damage. The accumulation of the former, on the contrary, is related to damage growth through a suitable function. The trend of such a function is governed by a key parameter, namely f_1 , which has to be carefully identified in order to get the proper ratio between energies spent in irreversible straining and in elastic stiffness degradation respectively (see Ferrara and di Prisco, 2000). Damage is kept, as in Mazars' original idea (1984) as a scalar variable, whose evolution is controlled by a suitably defined strain invariant, given by the positive parts of the strain tensor. According to Pijaudier-Cabot and Bazant (1987), the non-local counterpart of such a local strain invariant is built through a suitable spatial averaging – in order to properly embed the non-local feature into the model formulation. This actually introduces an internal length scale l_c , which is closely connected to the degree of material heterogeneity (i.e., characteristic length, maximum aggregate size). As a matter of fact the evolution of such a scalar variable is actually regarded as the outcome of three different modes of "positive straining" (cracking). A direct damage mode, driven by positive tensile stresses, hence aligned with the tensile strains themselves, is distinguished from an indirect one, driven by compressive stresses, which are at right angles to the cleavage strains. The corresponding behaviors are combined into a unique damage evolution law through suitable "weighting functions", which, in the enhanced formulation proposed by Ferrara (1998) is represented by two internal variables. They are in fact built up, step by step, from the positive work done by tensile (direct damage) and compressive stresses (indirect damage).

The "Crush-Crack" damage model therefore requires, as an input, the description of the constitutive material behavior – in terms of stress-strain laws – under the three basic load conditions – namely uniaxial tension, uniaxial and biaxial compression – which are associated to the three basic damage evolution laws.

Uniaxial compressive behavior was modeled as suggested by the CEB-MC90; biaxial compressive response has been described through the same relationships provided a biaxial strength value and a

biaxial peak strain both equal to 1.2 times the respective uniaxial parameters and a biaxial Young's modulus equal to $E/(1-\nu)$ are assigned.

The pre-peak uniaxial tension behavior has been modeled by means of a third-order parabola, having a zero slope at the peak. Post-peak behavior has been described as bilinear; the ultimate strain ϵ_u being set equal to $5.14 \frac{G_t}{f_t h}$ - analogous to Hordijk's

exponential softening law, where G_f is the mode I fracture energy of concrete and h is the characteristic length, equal to the maximum aggregate size (di Prisco et al., 1999). The breakpoint coordinates have to be calculated by simultaneously satisfying the following conditions:

$$g_{f1} + g_{fII} = g_R$$

$$g_{f1} = g_{fII} \text{ for NSC}$$

$$\text{or } g_{f1} = 2 g_{fII} \text{ for HSC}$$

where $g_R = G_f/h$ and g_{f1} and g_{fII} are the areas subtended, respectively, by the first and second branches of the input softening law.

For fiber-reinforced concrete, the uniaxial tensile behavior has been described as (see Figure 1):

- pre-peak is the same as in the reference plain concrete;
- a tri-linear post-peak, with:
 - the first steepest branch coinciding with the reference plain concrete (the coordinates are computed by means of proportionality ratios, taken for the upward shift of the curve due to the fiber residual stress);
 - the second branch is parallel to the second softening branch of the reference plain concrete but shifted upward by a quantity equal to the fiber concrete residual stress
 - the third horizontal branch, where the stress is equal to the residual strength in tension, σ_{res} .

Compressive behavior has been described by suitably modifying Saenz's formula in the post-peak region and in such a way that the curves have an horizontal asymptote $\sigma = \sigma_{res,c}$. Residual strength in compression is determined such that the $\sigma_{res,c}/f_c$ ratio is exactly equal to that of $\sigma_{res,t}/f_t$.

A correct, effective and physically sound identification of the residual strength in tension is the basis for the modeling tool proposed here for the FRC behavior. It has been suggested in a previous work (Ferrara and Gettu, 2000) that this should be obtained from flexural test results, through suitable hypotheses regarding the crack opening, by means of simple energy equivalence conditions, while maintaining the validity of the hypotheses used for the reference plain concrete, which permits the transfer of experimental results to the smeared crack framework. It has to be noted that the presence of fibres is

likely to modify the degree of heterogeneity of the material; its characteristic length should not, therefore, be related only to the maximum aggregate size only but should also take the length of fibers into account. The exact quantification of such an influence needs a wide experimental and numerical study, with the proper calibration of a variable characteristic length, which would be better for representing the different stages of activation of the fiber contribution. Since no such studies exist, it has been decided in this work to adopt the hypothesis widely used for plain concrete, and to set the characteristic length equal to the maximum aggregate size.

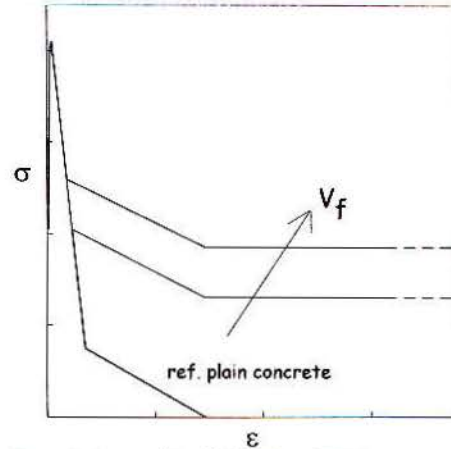


Figure 1: Assumed tensile behavior of FRC

The entire set of the above-mentioned hypotheses has been checked by analyzing a series of three point bending tests. Two different series of tests have been taken into account: tests on high strength concrete (HSC) performed by Carmona (1997) and tests on fiber reinforced concrete (FRC) with three different percentages of fibers (0%, 0.5% and 1% by volume) performed by Jamet et al., 1995. For each type of concrete, tests on beams of three different sizes have been modeled so as to have an insight into the capabilities of the model to reproduce the size dependence of the fracture behavior of concrete.

Figure 2 shows the geometry of the analyzed specimens as well as the meshes employed in the analyses. It is worth remarking that, in order to have a correct reproduction of the size dependent material behavior, the same number of elements inside the non-local averaging support, close to the notch tip and along the fracture plane, has been chosen for the different beam sizes. The diameter of such an averaging support is set by the code as thrice the internal length scale l_c , mentioned earlier. Previous parametric analyses have shown that such a length is closely linked to the material characteristic length h , the ra-

ratio between h and l_c being, for all the above mentioned modeling assumptions, equal to 5.5 (Ferrara and di Prisco, 2001).

In Table I, the material properties assumed in the analyses have been summarized. In both cases, twice the value obtained experimentally through the Size Effect Method has been assumed for the fracture energy.

Table I: material parameters

	HSC	FRC
f_c	61 MPa	72 MPa
E_c	35.2 GPa	40 GPa
f_t	3.75 MPa (CEB-MC90)	4.1 MPa
G_F	89.2 N/mm	70 N/mm
h	12 mm (= d_s)	12 mm (= d_s)
		σ_{res} 1.3 MPa (FRC 0.5)
		σ_{res} 1.85 MPa (FRC 1.0)

The reliability of the modeling assumptions is clearly reflected in the satisfactory fit of the experimental results, in terms of load vs. CMOD curves, for plain and fiber concretes (Figures 3-4).

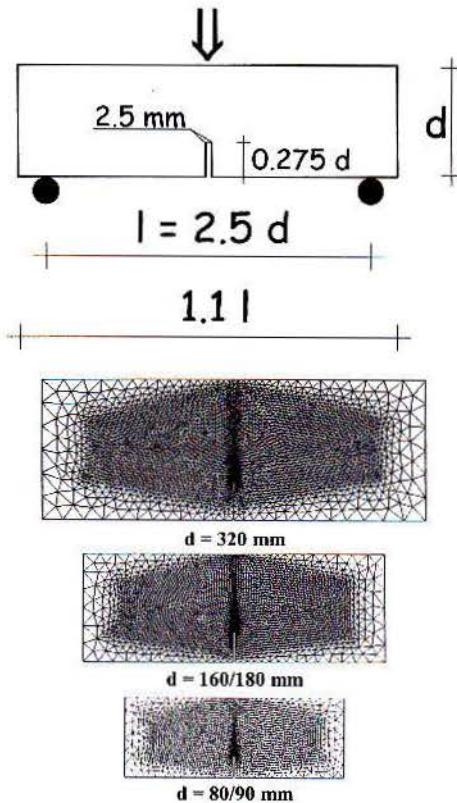


Figure 2. Geometry of the 3pb specimen and the meshes employed.

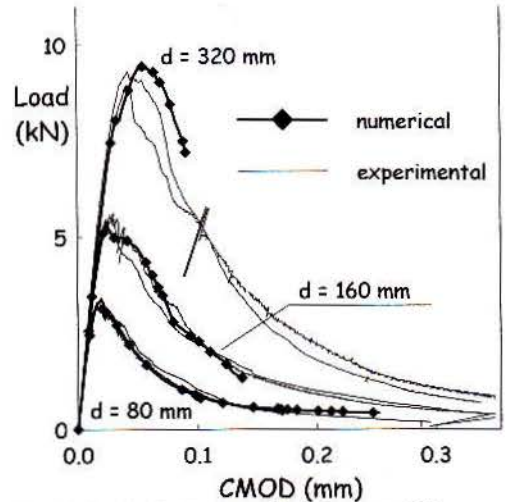


Figure 3: Load - CMOD curves for 3pb tests on HSC

3 MODELLING SPLITTING TESTS OF WHOLE AND HALVED DISKS

The modeling tool proposed and checked in the previous section has been applied in the analysis of splitting tests of both whole and halved disks (Carmona et al., 1998). Due to the uncoupling of the resistant mechanisms that the “double” test configuration permit, such tests may be regarded as suitable references for an improved calibration of model parameters, mainly for the coupling of direct and indirect damage.

In Figure 5, the meshes employed for the analyses of both the whole and the halved disks are shown; for the latter actually a 1 μ m wide cut was modeled between the two parts, imposing unilateral constraints on the horizontal displacements of points on the two diameters. For the analyses of splitting disks of various diameters, the same number of elements inside the non-local averaging support ($\approx 3l_c$) has been used in the process zone, i.e. along the vertical diameter.

Figure 6 shows the load vs. COD curves for the halved disks of four different diameters. The analysis seems to reproduce the trend of the curves, in a reasonable fashion, as well as to capture the maximum load, i.e. the bearing capacity of the two column-like half disks. The discrepancies between the experiments and numerical predictions may be attributed to the boundary conditions, which cannot be exactly reproduced in the analyses. For example, some friction between the halved disks and the cardboard loading strips, placed between the specimen and the loading bars, may lead to large variations in the stiffness, as seen in the experiments, as well as the higher load recorded for the smaller disk ($\phi = 74$ mm). The presence of cardboard may have also in-

fluenced the global load bearing capacity in the following way. A progressive activation of the contact pressure over the load application width may be responsible for the lower recorded load for larger disks.

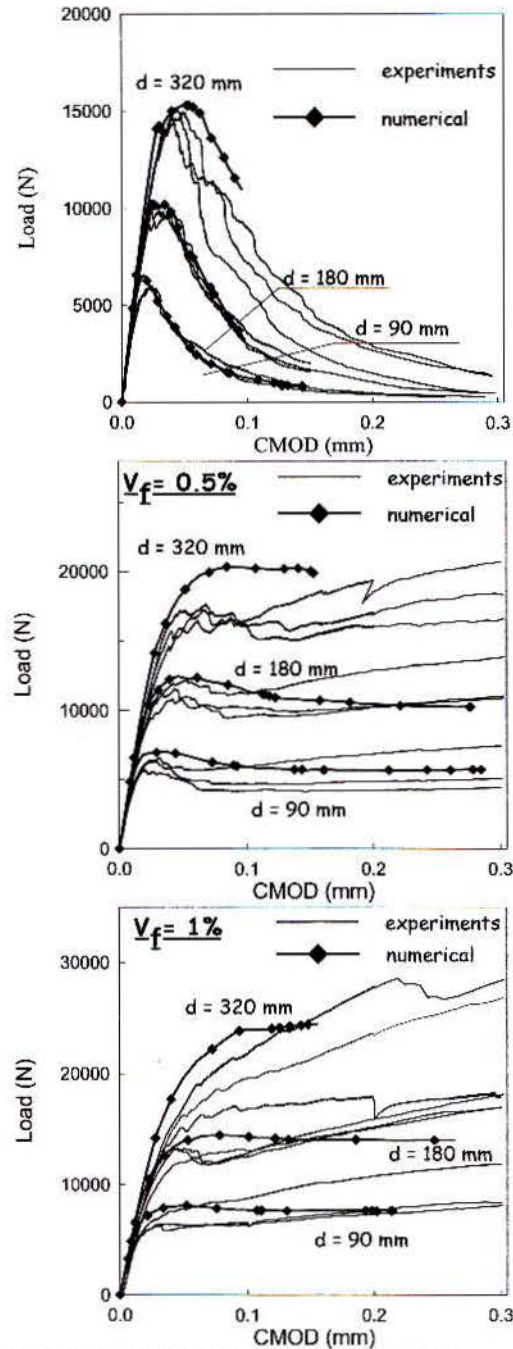


Figure 4. Load vs. CMOD curves for 3pb tests on FRCs

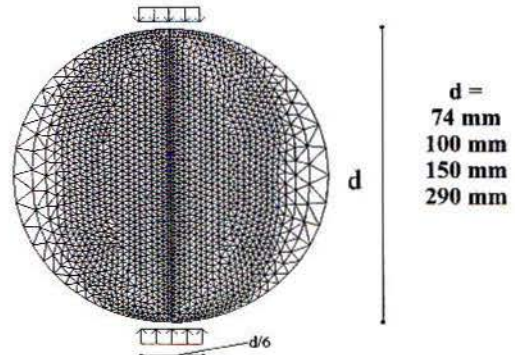


Figure 5. Example of mesh for splitting disks ($d = 150$ mm)

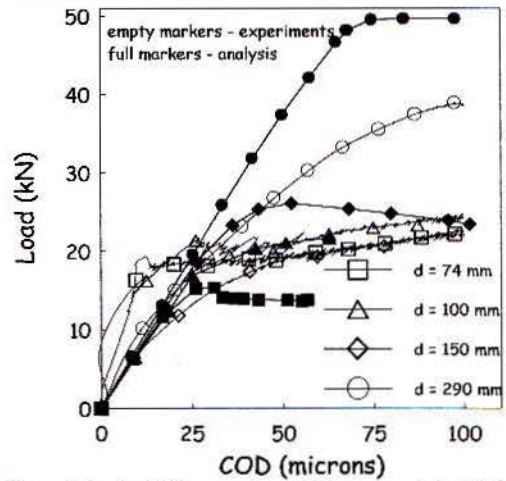


Figure 6. Load - COD curves for splitting tests on halved disks

Early loss of convergence for numerical analyses may be attributed to the possible activation of some rigid body movements along the horizontal direction. The half-disks were in fact left free to move along that direction, in order to prevent any spurious passive confinement, strongly modifying the kinematics of the system, as some analyses have shown. A parametric analysis of the influence of horizontal boundary conditions on the behavior of such a specimen should be performed, which would be also helpful at better clarifying the influence eventually played by friction with cardboard and by the boundary conditions in general. Nevertheless, the analyses reproduce the crack pattern well (see Figure 7), with cracks starting from the corners of the load application strips, and tending to propagate vertically or inclined, towards the vertical diameter so to form the typical wedges. As far as the size dependent features of the failure the halved disk system are concerned, the analyses seem to confirm a strong size dependence for smaller sizes and an almost negligible one for diameters larger than 150 mm, even with some quantitative difference with respect to the experiments.

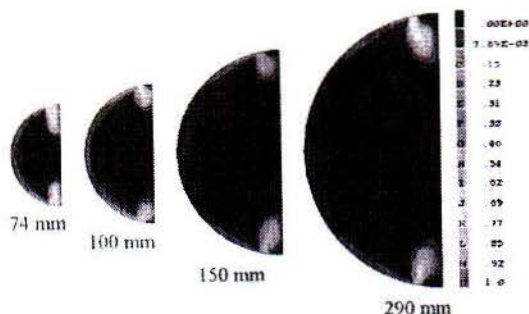


Figure 7. Damage patterns (end of calculation) - halved disks

Despite such differences, the analyses also show that the failure of the half-disks is rather ductile, with moderate softening, in some cases, which may also be attributed to the boundary conditions in the horizontal direction. This aspect, as well as the trend of the load-COD curves, suggests that, in the splitting tests, the region of the vertical diameter undergoes increasing or almost constant vertical stresses while the horizontal stresses decrease as the diametral crack forms and propagates. This continuous input of elastic stored energy into a zone close to the fracture process may explain the size dependence of the splitting strength observed in the experiments (Carmona et al., 1998). This has been analyzed in the case of the whole disks using the results, in terms of load vs. crack opening curves, shown in Figure 8, for HSC, and in Figure 9, for FRC. The crack opening was measured over a 65 mm gauge length at the center of the specimen. The analyses, as can be seen, underestimate the maximum loads, for both HSC and FRC specimens. In the latter, the hardening post-peak trend is reproduced in the analyses. The underestimation of the peak load can be attributed to different causes. Along the vertical diameter, in a splitting disk, tensile strains are generated, due to both tensile and compressive stresses. The model, due to its scalar damage formulation, computes damage evolution on the basis of a positive strain invariant, which, obviously, does not distinguish between the strains due to positive or negative stresses, taking into account only the total value. This may cause the damage evolution to be computed faster than it actually is, lowering the numerical maximum load as in Figure 10, as well as causing the early formation of the wedges below the loading platens, which was observed in the experiments to occur only after the complete formation of the vertical crack. The inability to simulate the true boundary conditions may also have played a non-negligible role. Moreover, it can be seen, from the horizontal and vertical stress patterns along the vertical diameter in Figure 11, that the input tensile

strength is never attained, with the maximum computed tensile stress being roughly equal to 2/3 of the assigned value. The "solution" of adopting a larger tensile strength has not been pursued since it is not in agreement with calibration with the 3pb beams.

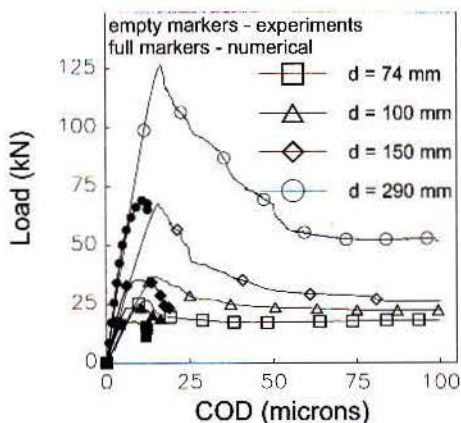


Figure 8. Load-COD curve for splitting tests on HSC disks.

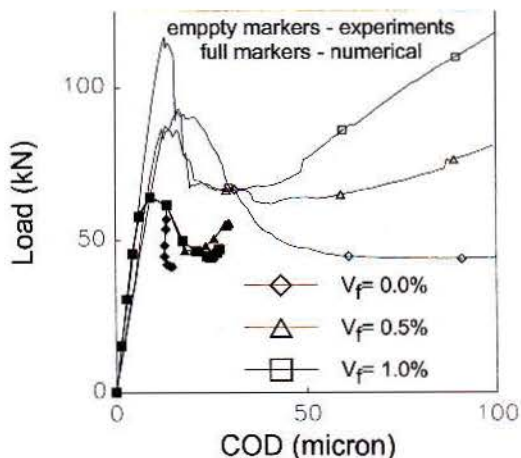


Figure 9. Load - COD curves for splitting tests on FRC disks.

4 CONCLUDING REMARKS

Size dependence of splitting strength seems to be governed by two parallel acting mechanisms, the splitting tension and the compressive bearing capacity of the specimen halves. The latter increases and continues to store elastic strain energy while fracture proceeds along the vertical diameter plane. This could explain the size independence of the failure stress in the splitting disks. The proposed tool for modeling FRC behavior has been proven to be quite effective and results of three point bending analyses confirm such a reliability. The crush-crack non-local damage model, while reasonably reproducing the analyzed tests splitting tensile tests from a qualita-

tive point of view, has underestimated the maximum load. The uncoupling of positive strains associated with tensile and compressive stresses, in the evaluation of damage evolution laws, has been used for the enhancement of the model formulation. A careful check of the influence of the boundary conditions on the test results seems to be essential.

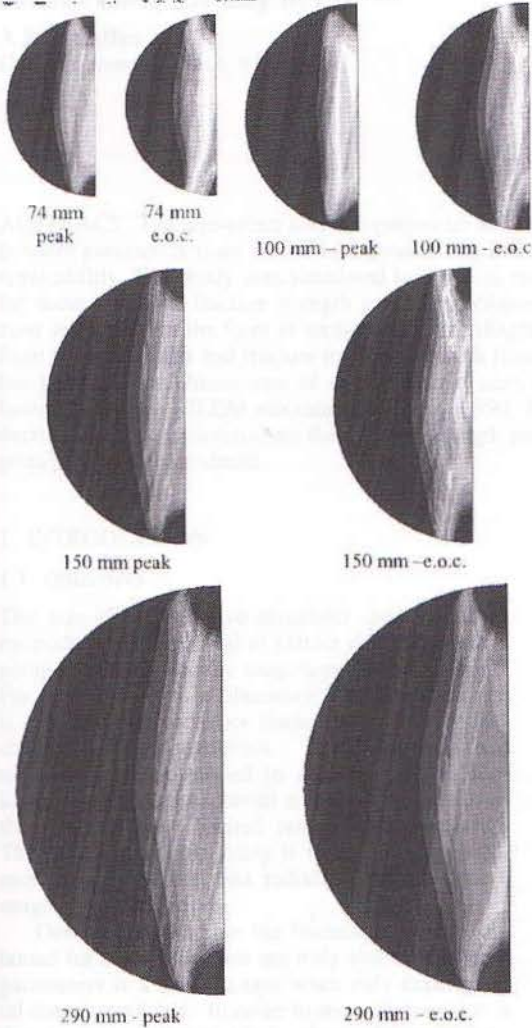


Figure 10. Damage patterns for HSC disks

ACKNOWLEDGEMENTS

The financial support of Italian Ministry for University and Scientific/Technological Research within the project "The post cracked behavior of FRC concrete: Identification tests and their design meaning" is gratefully acknowledged. The collaborative research was made possible by a Joint Spain-Italy project Acción Integrada (HI 1997-0219).

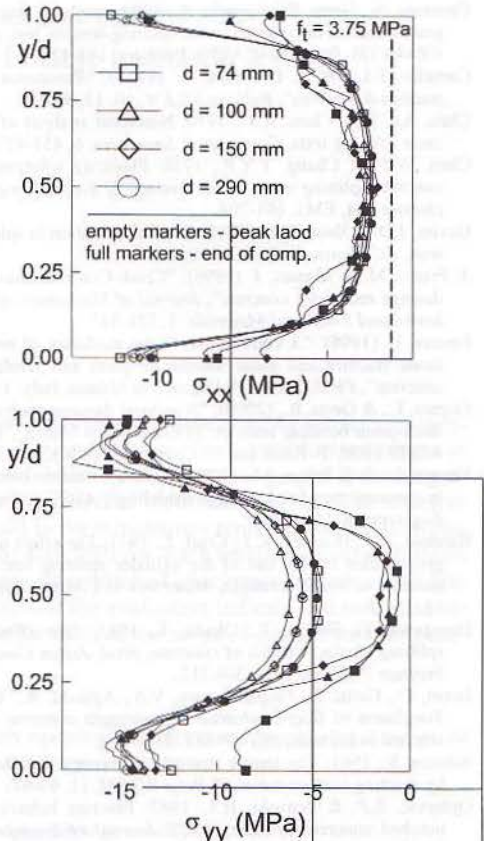


Figure 11. Stress patterns along the vertical diameter

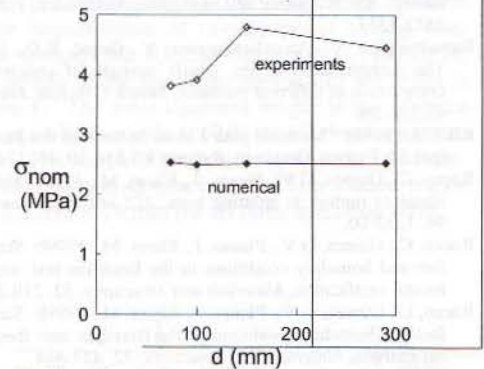


Figure 12: Size effect on the splitting strength

REFERENCES

Bazant, Z.P., Kazemi, M.T., Hasegawa, T., Mazars, J., 1991: Size effect in brazilian split-sylinder tests: measurements and fracture analysis, *ACI Materials Journal*, 88, 3, 325-332.
 Carmona, S., 1997: Caracterización de la fractura del hormigon y de vigas de hormigon armado, *PhD Thesis*, UPC Barcelona, Spain.

- Carmona, S., Gettu, R., Aguado, A., 1998: Study of the post-peak behavior of concrete in the splitting-tension test, *Proc. FRAMCOS-3, AEDIFICATIO*, Freiburg, 111-120.
- Carneiro, F.L.L.B. & Barcellos, A. (1953): "Resistance a la traction des betons", *Bulletin RILEM*, 10, 13, 99-123.
- Chen, A.C.T. & Chen, W.F., 1976: Nonlinear analysis of concrete splitting tests, *Computer & Structures*, 6, 451-457.
- Chen, W.F. & Chang, T.Y.P., 1978: Plasticity solutions for concrete splitting tests, *ASCE Journal of Engineering Mechanics* 104, EM3, 691-704.
- Davies, J.D. & Bose, D.K., 1968: Stress distribution in splitting tests, *ACI Journal*, 65, 662-669.
- di Prisco, M. & Mazars, J. (1996): "Crush-Crack: a non-local damage model for concrete", *Journal of Mechanics. of Cohesive and Frictional Materials*, 1, 321-347.
- Ferrara, L. (1998): "A contribution to the modeling of mixed-mode fracture and shear transfer in plain and reinforced concrete", *Ph.D. Thesis*, Politecnico di Milano, Italy, 1-245.
- Ferrara, L., & Gettu, R., (2000): "Non-local damage analysis of three-point bending tests on SFRC notched beams", *Proc. BEFIB 2000*, P. Rossi and G. Chanvillard (eds.), 357-368.
- Ferrara, L., & di Prisco, M., (2001): "Mode I fracture behavior in concrete: non-local damage modeling", *ASCE Journal of Engineering Mechanics*
- Hannant, D.J., Buckley, K.J., Croft, J., 1973: The effect of aggregate size on the use of the cylinder splitting test as a measure of tensile strength, *Materiaux et Constructions*, 6, 31, 15-21
- Hasegawa, T., Shioya, T., Okada, T., 1985: Size effect on splitting tensile strength of concrete, *prod. Japan Concrete Institute 7th Conference*, 309.312.
- Jamet, D., Gettu, R., Gopalaratnam, V.S., Aguado, A., 1995: Toughness of fiber-reinforced high-strength concrete from notched beam tests, *ACI-SP 155*, 23-39.
- Nilsson, S., 1961: The tensile strength of concrete determined by splitting tests on cubes, *Bulletin RILEM*, 11, 63-67.
- Ojdrovic, R.P. & Petroski, H.J., 1987: Fracture behavior of notched concrete cylinder, *ASCE Journal of Engineering Mechanics*, 113, 10, 1551-1564.
- Pijaudier-Cabot, G., & Bazant, Z.P. (1987), 'Non-local damage theory', *ASCE Journal of Engineering Mechanics*, 113, 10, 1512-1533.
- Ramakrishnan, V., Ananthanarayana, Y., Gopal, K.C., 1967: The determination of the tensile strength of concrete: a comparison of different methods, *Indian Concrete Journal*, 41, 202-206
- RILEM, (1953): "Methode pour l'essai de traction des betons" (par M. Tsunéo Akazawa), *Bulletin RILEM*, 10, 16, 12-23.
- Rocco, C., Guinea, G.V., Planas, J., Elices, M., 1999a: Mechanisms of rupture in splitting tests, *ACI Materials Journal*, 96, 1, 52-60.
- Rocco, C., Guinea, G.V., Planas, J., Elices, M., 1999b: Size effect and boundary conditions in the Brazilian test: experimental verification, *Materials and Structures*, 32, 210-217.
- Rocco, C., Guinea, G.V., Planas, J., Elices, M., 1999b: Size effect and boundary conditions in the Brazilian test: theoretical analysis, *Materials and Structures*, 32, 437-444.
- Wright, P. J. F, 1955: "Comments on an indirect tensile test on concrete cylinders", *Magazine of Concrete Research*, 7, 20, 87-95.